Polymer Chemistry

ROYAL SOCIETY OF CHEMISTRY

COMMUNICATION

Cite this: DOI: 10.1039/d5py01006c

Received 23rd October 2025,
Accepted 21st November 2025

DOI: 10.1039/d5py01006c

rsc.li/polymers

Pressure-sensitive adhesives from polyester pentablock copolymers

Chang Gao, Kam C. Poon and Charlotte K. Williams *

Pressure sensitive adhesives (PSAs) are widely used materials in a number of applications, such as sticky notes and tapes, but for most commercial products they are derived from petrochemicals. Here, a series of pentablock polymers, with an ABABA structure featuring poly(cyclohexene oxide-*alt*-phthalic anhydride) 'A' blocks and poly(ε-decalactone) (PDL) 'B' blocks, are prepared as pressure-sensitive adhesives from bio-sourced monomers. The pentablock polymers are prepared by controlled polymerisation techniques, using a single catalyst, in a one-pot process. Polymer properties are tuned through varying the hard block (A) content between 16–39 wt%. Below 25 wt% hard block, the pentablock polymers show low-tack adhesive performance (0.2–0.6 N cm^{-1}) and are removed by adhesive failure. Their adhesive performance compares favourably to low-tack commercial adhesives.

Introduction

Pressure-sensitive adhesives (PSAs) are an important class of materials used as tapes, glues and labels in packaging, automotive components, and electronics.[1] They are characterised by their ability to self-adhere quickly under light pressure, resist shear forces during use, and be removed without leaving adhesive residue.[2–5] To achieve this, PSAs should have a balance between the viscous flow required for substrate wetting and elasticity for mechanical integrity and removability.[6] Most PSAs consist of polyacrylates, natural rubbers or styrenic copolymers which are combined with tackifier and other additives.[4,7–9] Amongst these formulations, tackified styrenic block copolymers stand out for their tuneable viscoelastic and mechanical properties. These materials are typically ABA triblocks which comprise 10–30 wt% of the hard/glassy 'A' block with a glass transition temperature (T_g) > room temperature and the remainder a soft/rubbery 'B' block (T_g < room temperature). Block phase separation is desirable, with the rubbery matrix enabling substrate wetting and surface contact, while the hard domains act as physical crosslinks to provide cohesive strength and resist shear forces.[4,10]

With the exception of natural rubber based-PSAs, most formulations are petrochemically derived (*e.g.* polyacrylates or styrenics). Development of alternative sustainable materials to the petrochemically sourced polymers is essential to reduce the 1.8 Gt of carbon dioxide (CO_2)-equivalents emitted annually from petrochemical polymer manufacturing.[11–15] Oxygenated block polymers offer attractive alternatives as they can be derived from renewable feedstocks and their high oxygen content should improve substrate adhesion.[16–18] Polyester-based PSAs are well precedented, with their potential established by Long and co-workers.[19–21] Triblock polyester PSAs made by cylic ester ring opening polymerisation (ROP) were initially demonstrated by Hillmyer and co-workers utilising monomers from biomass feedstocks; since then, many successful examples have been developed from renewable monomers such as lactide (from corn starch), menthide (from mint), and ε-decalactone (from castor oil).[22–30] In most cases, the block polymers require further formulation with additives and tackifiers to deliver the desired adhesive behavior. Although certain additives, such as rosin esters, can be renewably sourced, multi-component adhesives are inherently more complex, posing challenges for future recycling and waste management.

Single-component PSAs based on oxygenated block copolymers have been reported by our team and others.[31–35] These materials were accessed by switchable polymerisation catalysis which allows for coupling of ring opening copolymerisation (ROCOP) of epoxide with CO_2 or anhydride and cyclic ester ring opening polymerisation (ROP), using a single catalyst, in a one-pot process.[36,37] This highly controlled catalysis results in the production of block polyesters with predictable high molar masses, and monomodal distributions, with high end-group fidelity, and obviates the requirement for intermediary polymer purification steps.[38–41] Our prior reports utilise a heterodinuclear [Zn(II)Mg(II)] catalyst to produce ABA triblock

Chemistry Research Laboratory, Department of Chemistry, University of Oxford, OxfordOX1 3TA, UK. E-mail: charlotte.williams@chem.ox.ac.uk

polymers featuring CO_2-polycarbonate hard-blocks with poly(ε-decalactone) (PDL) mid-blocks.[32,42] Using the same catalysis, fully biobased polyester PSAs were synthesised from tricyclic anhydrides, limonene oxide, and ε-decalactone.[31] In both examples the oxygenated PSAs achieved high peel forces (2–13 N cm^{-1}) comparable to commercial tapes such as Duct tape or Scotch tape.

There is an industrial application for low-tack PSAs which are removable with a peel force around 0.5 N cm^{-1}.[26] In these applications, achieving adhesive failure is important for more temporary PSA applications, and this could be investigated through modification of the block structure. Adhesive failure occurs when the cohesive strength of the adhesive is greater than the interfacial adhesion to the substrate.[43] Targeting higher-order block polymer structures, such as a pentablock polymer, introduces additional hard domains which could act as physical crosslinks to increase the internal strength of the adhesive, promoting adhesive failure. Switchable polymerisation catalysis allows for controlled and selective sequencing of blocks which enables synthesis of higher-order multiblock polymers, for example pentablock or heptablock polymers.[42,44] Here, we investigate polyester-based pentablock copolymers and their potential as pressure-sensitive adhesives. They have an ABABA structure, with poly(ε-decalactone) (PDL) soft 'B' blocks and poly(cyclohexene oxide-*alt*-phthalic anhydride) (P(CHO-*alt*-PA)) hard 'A' blocks. The pentablocks are prepared from bio-derived monomers: ε-decalactone (castor oil),[45,46] cyclohexene oxide (waste plant oil),[47,48] and phthalic anhydride (corn stover).[49,50] The adhesive properties of these materials are studied to understand how block architecture might influence adhesion strength and failure mechanism.

Results and discussion

A series of ABABA pentablock copolymers featuring semi-aromatic poly(cyclohexene-*alt*-phthalate) (PE) A-blocks in combination with poly(ε-decalactone) (PDL) B-blocks were synthesised in a one-pot procedure using sequential monomer addition. Polymerisations were conducted using the $[LZnMg(C_6F_5)_2]$ heterodinuclear catalyst, at 100 °C, with 1,4-benzenedimethanol (BDM) as an alcohol initiator (Fig. 1 and Fig. S1).[51–53] The catalyst system was reacted with a monomer mixture initially comprising phthalic anhydride (PA), cyclohexene oxide (CHO), and ε-decalactone (DL) ($[[LZnMg(C_6F_5)_2]_0 : [BDM]_0 : [\varepsilon\text{-DL}]_0 : [PA]_0 : [CHO]_0$ = 1 : 2 : 1000 : 153 : 690). The ring-opening copolymerisation (ROCOP) of PA and CHO takes place first, to form the central P(PA-*alt*-CHO) block after 2 h (>99% conversion, TOF = 77 h^{-1}). The reaction progress was monitored by ^{1}H NMR spectroscopy of a reaction aliquot through comparison of the relative integrals of the aromatic resonances in PA (7.99 ppm) and P(CHO-*alt*-PA) (7.59 ppm) (Fig. S2). Following complete consumption of the PA in the initial monomer mixture, there is a mechanistic switch from ROCOP to ring-opening polymerisation (ROP) of DL to afford the PDL-P(PA-*alt*-CHO)-PDL copolymer. After 16 h, the DL ROP was complete (97% conversion, TOF = 60 h^{-1}), as confirmed by ^{1}H NMR spectroscopy by comparison of the relative integrals of the –CH resonances in DL (4.27 ppm) with PDL (4.91 ppm). To achieve the desired pentablock copolymer structure, a second portion of PA (307 equiv.) was added into the reaction mixture to grow the outer hard blocks. After 72 h, the second ROCOP was complete (>99% conversion, TOF = 4 h^{-1}), resulting in selective P(PA-*alt*-CHO)-PDL-P(PA-*alt*-CHO)-PDL-P(PA-*alt*-CHO) pentablock formation. The slower rate observed for the second ROCOP likely

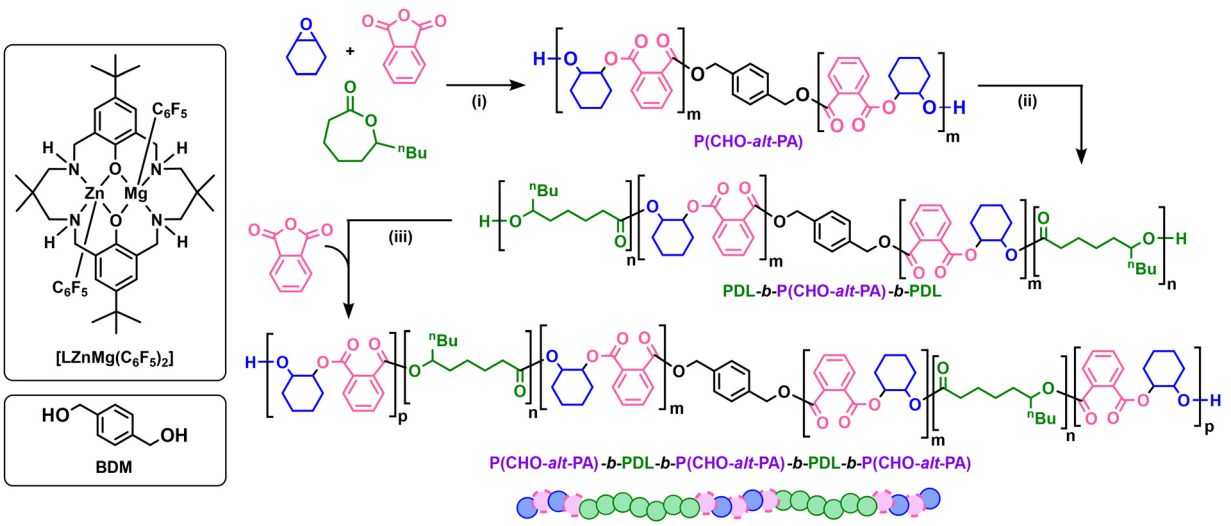

Fig. 1 Synthesis of the pentablock polyesters by sequential monomer addition. $[LZnMg(C_6F_5)_2]_0 : [BDM]_0 : [\varepsilon\text{-DL}]_0 : [PA]_0 : [CHO]_0$ = 1 : 2 : 1000 : 460 : 690. $[CHO]_0$ in toluene = 1.5 M. Note that the PA is added in two portions with relative amounts 153 (i) and 307 equiv. (iii), in each case amounts are *vs.* catalyst. (i) PA/CHO ROCOP at 100 °C catalysed by $[LZnMg(C_6F_5)_2]$ with BDM as a bifunctional initiator to form P(CHO-*alt*-PA) homopolymer. (ii) DL ROP at 100 °C forming PDL-P(CHO-*alt*-PA)-PDL triblock copolymer. (iii) Second addition of PA followed by PA/CHO ROCOP at 110 °C to form P(CHO-*alt*-PA)-PDL-P(CHO-*alt*-PA)-PDL-P(CHO-*alt*-PA) pentablock copolymer.

arises from decreased accessibility of chain ends at higher molecular weight and the lower concentration of CHO as the monomer is consumed. The reaction mixtures were quenched by exposure to air, followed by removal of catalyst and isolation of the polymer by precipitation into methanol. The polymers were dried under vacuum to remove all residual solvent (150 °C, 24 h). ^{1}H NMR spectroscopy and thermogravimetric analysis (TGA) helped confirm the complete removal of the processing solvents and catalyst (Fig. S2 and S8–11).

Selective formation of the block polyester is supported by SEC analysis of reaction aliquots which show a steady increase in polymer molar mass (M_n) through the reaction from around 10 kg mol^{-1} to 50 kg mol^{-1} to 70 kg mol^{-1} whilst retaining a monomodal distribution of moderate dispersity ($Đ$ < 1.4) (Fig. S5). ^{1}H DOSY NMR analysis of the pentablock polymer also shows a single diffusion coefficient for all resonances, suggesting all blocks are joined (Fig. S6). Analysis of the chain-end groups, by ^{31}P{^{1}H} NMR spectroscopy following treatment with a phospholane reagent, showed only the presence of P(CHO-*alt*-PA) hydroxy end-groups (146.4 ppm) from the outer hard block (Fig. S7).[54] Analysis of the carbonyl region of the ^{13}C{^{1}H} NMR spectra shows signals for both the P(CHO-*alt*-PA) and PDL blocks at 166.8 ppm and 173.4 ppm, respectively (Fig. S3). This is consistent with block polymer formation without transesterification block scrambling.[55]

Four pentablock copolymers (**PB-1** to **PB-4**) were synthesised with approximately the same M_n (~70 kg mol^{-1}) but show increasing hard block content from 16 to 39 wt% (Table 1). Accessing high molecular weight polyesters, particularly through using ROCOP and switch catalysis, remains challenging showcasing the excellent performance of the Zn(II)Mg(II) catalyst.[56,57] Relatively lower hard block contents were chosen to allow enough soft block needed for surface wetting and tack in PSAs.[4] The relative hard block wt% was determined from the relative integrals of the PDL block resonance (4.85 ppm) to the P(CHO-*alt*-PA) resonance (7.58 ppm) (Fig. S2). Differential scanning calorimetry (DSC) shows the polymers are all amorphous, showing a lower glass transition temperature (T_g) close to −50 °C and upper T_g of 138 °C (Fig. S12). The T_g values observed are close to the expected values for the constituent polymers suggesting phase separation of the hard and soft blocks.[51,58–60] The apparent absence of an upper T_g by DSC in samples with low hard block content (**PB-1** and **PB-2**) is due to its reduced concentration and low DSC signal intensity.[32,51,52]

Small-angle X-ray scattering (SAXS) data of films of **PB-3** and **PB-4** show a principal scattering peak (q^*) with domain spacing (d) of 20 nm and 26 nm, respectively (Fig. S14). The SAXS data is consistent with phase separation, but long-range ordering is limited as higher-order peaks are not observed for the pentablock polymers. TGA showed relatively high thermal stability compared with other polyesters and with the onset to decomposition occurring at $T_{d,5\%}$ ≥ 310 °C for all polymers (Fig. S8–11). **PB-3** and **PB-4** could be processed into free-standing films. In contrast, **PB-1** and **PB-2**, which have low hard block content (<20 wt%), are highly viscoelastic and unable to form freestanding films.

Rheological frequency sweeps were performed to assess the viscoelastic properties across the series of polymers (Fig. 2a and Fig. S15–17). From this, a viscoelastic window was constructed using the shear storage modulus (G') and shear loss modulus (G'') at frequencies consistent with adhesive bonding (10^{-1} rad s^{-1}) and debonding (10^{2} rad s^{-1}) for each pentablock polymer (Fig. 2b).[61,62] For adhesives these values are an important measure of the response of a material to shear forces during application and removal.[1] G' at the bonding frequency must fall below the Dahlquist criterion ($G' \leq 3 \times 10^5$ Pa) to promote good adhesive contact due to surface wetting.[2] This is true for samples **PB-1**, **PB-2**, and **PB-3**, which show G' values below the Dahlquist criterion, indicating they should be effective PSAs without the need for additives or tackifiers. The bonding modulus of **PB-4** lies above the Dahlquist criterion, which is likely a result of the higher hard block content (39 wt%), rendering the material too rigid to be considered a PSA. For comparison, the equivalent triblock copolymer (**TB-1**) with 25 wt% hard block, shows a bonding modulus above the Dahlquist criterion, indicating the material is too stiff to be considered a PSA (Fig. S18–19).[51] The application potential of the pentablock polyesters was assessed according to Chang's quadrant method.[1] The viscoelastic windows of **PB-1** and **PB-2** suggest they should be easily removable PSAs, whereas, **PB-3** falls within the window of general-purpose PSAs.

Samples **PB-1**, **PB-2**, and **PB-3** were assessed as pressure sensitive adhesives by 180° peel tests, using polished stainless steel as the substrate and PETE film (Mylar) as the adhesive backing (ISO 29862:2018). Peel adhesions for **PB-1** (0.19 N

Table 1 Pentablock polyester characterisation data

Sample	wt % PDL : P(PA-*alt*-CHO)[a]	$M_{n,SEC}$[b,c] (kg mol^{-1}) [$Đ$]	T_{g1}, T_{g2}[d] (°C)	$T_{d,5\%}$[e] (°C)	Classification
PB-1	84 : 16	67 [1.26]	−48, n.o.	314	Viscoelastic liquid
PB-2	80 : 20	58 [1.20]	−49, n.o.	310	Viscoelastic liquid
PB-3	74 : 26	74 [1.27]	−49, 138	312	Elastomeric
PB-4	61 : 39	69 [1.36]	−48, 138	311	Elastomeric
TB-1[51]	76 : 24	89 [1.05]	−41, 136	307	Elastomeric

[a] Determined from the ^{1}H NMR spectra of purified samples (Fig. S2, SI). [b] Estimated by SEC with THF eluent, RI detector, calibrated using PS standards. [c] M_w/M_n. [d] Determined by DSC, second heating curve. n.o. = not observed. [e] Thermal degradation is reported as the temperature at which 5% mass is lost by TGA.

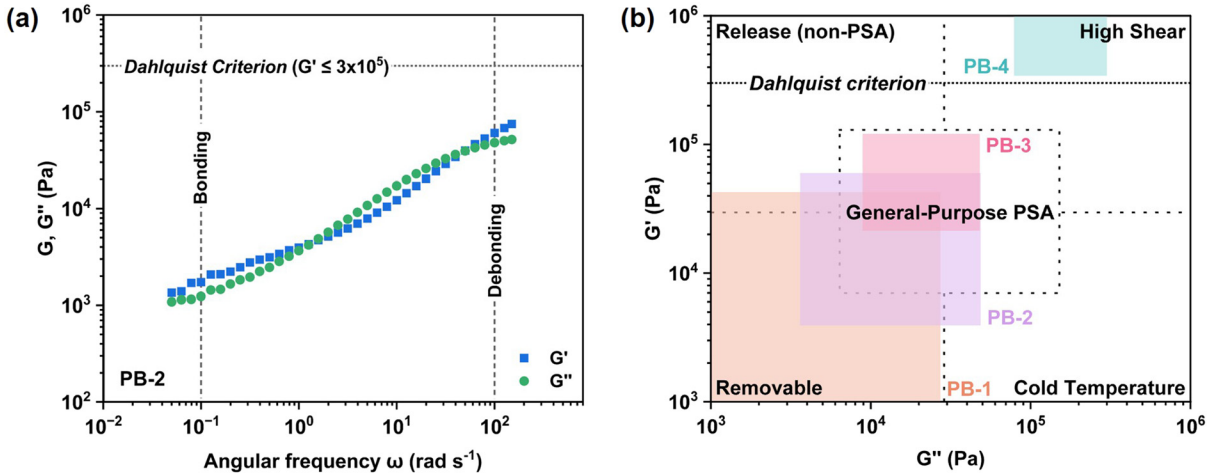

Fig. 2 (a) Frequency sweep of **PB-2** (25 °C). (b) PSA performance windows of pentablock polyesters constructed from the bonding (ω = 0.1 rad s^{-1}) and debonding frequencies (ω = 100 rad s^{-1}).

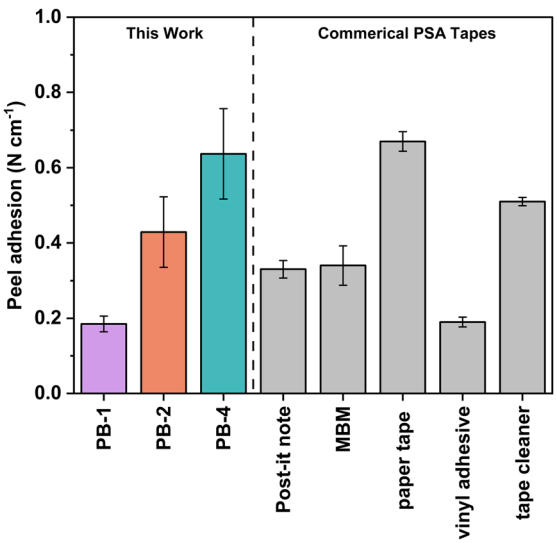

Fig. 3 180° Peel adhesion properties on stainless steel substrates of **PB-1**, **PB-2**, and **PB-3** with comparisons to commercial low tack PSAs.

cm^{-1}), **PB-2** (0.43 N cm^{-1}), and **PB-3** (0.64 N cm^{-1}) showed an increase with greater P(CHO-*alt*-PA) hard block content (16 to 26 wt%) across the series (Fig. 3). **PB-1** and **PB-2** demonstrated desirable adhesive failure with clean removal and no residue (Fig. S20). **PB-3** failed cohesively, leaving polymer residue on the substrate, which would be a disadvantage for a removable application. Adhesive failure results from bridging of the hard domains by the rubbery soft block in the block copolymers, which form fibrils during PSA debonding and increase cohesive strength of the PSA.[28,63] The lower hard block content of **PB-1** and **PB-2** promotes effective fibril formation and elongation during the PSA debonding, leading to adhesive failure. Whereas, this mechanism is more hindered in **PB-3**, which has higher hard block content, and resulted in cohesive failure. The low adhesion force of these materials is comparable to reported values for commercial low tack PSAs used for removable/repositionable tapes or surface protection films, such as MBM (0.34 N cm^{-1}), Post-it note (0.33 N cm^{-1}), low tack paper tape (0.67 N cm^{-1}), low tack vinyl adhesive (0.19 N cm^{-1}), and 3M tape cleaner (0.51 N cm^{-1}).[26] The pentablock polyesters provide low strength peel adhesion without the need for additional of additives such as tackifiers for PSA applications.

The stress–strain behaviour of **PB-3** and **PB-4** were studied by uniaxial tensile testing, at an extension rate of 10 mm min^{-1} (Table S2 and Fig. S21). Dumbbell shaped specimens were cut from the polymer films, according to ISO 527-2, specimen type 5B using a cutting press. **PB-3** and **PB-4** both exhibit elastomeric behaviour. **PB-3** shows low ultimate tensile strength (0.76 MPa) and a strain at break of 261%. At increased hard block content, **PB-4** showed an improvement in tensile strength (2.61 MPa) and strain at break (405%). PSAs with higher hard block content often have a G' that is too large, hindering substrate wetting and tackiness and thus limiting adhesive performance of **PB-4**.

A series of pentablock polymers with high molar mass and increasing hard block content were selectively prepared using a single catalyst, in a one-pot procedure. Polymerisations were highly controlled and selective, enabling the formation of multiblock polymers at varying block compositions. The polyesters were effective low-tack pressure sensitive adhesives, without the addition of tackifier resin or additives. They showed comparable adhesive performance to existing commercial materials, with favourable adhesive failure at lower hard block content (< 20 wt%) making them most suitable for temporary applications. These results showcase the utilisation of switchable catalysis to selectively prepare pentablock polymers which act as effective low-tack PSAs. It is expected that further manipulation of polymer composition, molar mass, and block ratios would allow further tuning of material properties.

Conflicts of interest

There are no conflicts to declare.

Data availability

The data that supports the findings of this study are available at: https://doi.org/10.5287/ora-9er8bzxvm.

Supplementary information (SI): experimental methods, spectroscopic data and thermal–mechanical data. See DOI: https://doi.org/10.1039/d5py01006c.

Acknowledgements

The EPSRC SCHEMA Hub (EP/Z532782/1, C. K. W. supporting K. C. P.), EPSRC (EP/S018603/1, C. K. W.) and the EPSRC Oxford Inorganic Chemistry for Future Manufacturing (OXICFM) Centre for Doctoral Training (EP/S023828/1 to C. K. W. supporting K. C. P. and C. G.) are acknowledged for research funding.

References

1 I. Benedek, *Pressure-Sensitive Adhesives and Applications*, CRC Press, Boca Raton, 2nd edn, 2004.
2 A. Zosel, *Colloid Polym. Sci.*, 1985, **263**, 541–553.
3 A. J. Crosby and K. R. Shull, *J. Polym. Sci., Part B:Polym. Phys.*, 1999, **37**, 3455–3472.
4 C. Creton, *MRS Bull.*, 2003, **28**, 434–439.
5 D. M. Fitzgerald, Y. L. Colson and M. W. Grinstaff, *Prog. Polym. Sci.*, 2023, **142**, 101692.
6 T. R. Ewert, A. M. Mannion, M. L. Coughlin, C. W. Macosko and F. S. Bates, *J. Rheol.*, 2018, **62**, 161–170.
7 K. R. Albanese, Y. Okayama, P. T. Morris, M. Gerst, R. Gupta, J. C. Speros, C. J. Hawker, C. Choi, J. R. de Alaniz and C. M. Bates, *ACS Macro Lett.*, 2023, **12**, 787–793.
8 M. A. Droesbeke, R. Aksakal, A. Simula, J. M. Asua and F. E. Du Prez, *Prog. Polym. Sci.*, 2021, **117**, 101396.
9 I. Khan and B. T. Poh, *J. Polym. Environ.*, 2011, **19**, 793–811.
10 J. Comyn, *Adhesion Science*, The Royal Society of Chemistry, London, 2nd edn, 2021.
11 J. Zheng and S. Suh, *Nat. Clim. Change*, 2019, **9**, 374–378.
12 F. M. Haque, J. S. A. Ishibashi, C. A. L. Lidston, H. Shao, F. S. Bates, A. B. Chang, G. W. Coates, C. J. Cramer, P. J. Dauenhauer, W. R. Dichtel, C. J. Ellison, E. A. Gormong, L. S. Hamachi, T. R. Hoye, M. Jin, J. A. Kalow, H. J. Kim, G. Kumar, C. J. LaSalle, S. Liffland, B. M. Lipinski, Y. Pang, R. Parveen, X. Peng, Y. Popowski, E. A. Prebihalo, Y. Reddi, T. M. Reineke, D. T. Sheppard, J. L. Swartz, W. B. Tolman, B. Vlaisavljevich, J. Wissinger, S. Xu and M. A. Hillmyer, *Chem. Rev.*, 2022, **122**, 6322–6373.
13 F. Vidal, E. R. van der Marel, R. W. F. Kerr, C. McElroy, N. Schroeder, C. Mitchell, G. Rosetto, T. T. D. Chen, R. M. Bailey, C. Hepburn, C. Redgwell and C. K. Williams, *Nature*, 2024, **626**, 45–57.
14 R. Geyer, J. R. Jambeck and K. L. Law, *Sci. Adv.*, 2017, **3**, e1700782.
15 G. Hayes, M. Laurel, D. MacKinnon, T. Zhao, H. A. Houck and C. R. Becer, *Chem. Rev.*, 2023, **123**, 2609–2734.
16 A. J. Teator and F. A. Leibfarth, *Science*, 2019, **363**, 1439–1443.
17 J. C. Foster and R. K. O'Reilly, *Science*, 2019, **363**, 1394–1394.
18 D. M. Krajovic, M. S. Kumler and M. A. Hillmyer, *Biomacromolecules*, 2025, **26**, 2761–2783.
19 G. I. Ozturk, A. J. Pasquale and T. E. Long, *J. Adhes.*, 2010, **86**, 395–408.
20 R. Abu Bakar, J. L. Keddie and P. J. Roth, *ChemPlusChem*, 2024, **89**, e202400034.
21 J. Li, Q.-Y. Zhang and X.-B. Lu, *Angew. Chem., Int. Ed.*, 2023, **62**, e202311158.
22 J. Shin, M. T. Martello, M. Shrestha, J. E. Wissinger, W. B. Tolman and M. A. Hillmyer, *Macromolecules*, 2011, **44**, 87–94.
23 K. Ding, A. John, J. Shin, Y. Lee, T. Quinn, W. B. Tolman and M. A. Hillmyer, *Biomacromolecules*, 2015, **16**, 2537–2539.
24 S. Lee, K. Lee, Y.-W. Kim and J. Shin, *ACS Sustainable Chem. Eng.*, 2015, **3**, 2309–2320.
25 H. J. Kim, K. Jin, J. Shim, W. Dean, M. A. Hillmyer and C. J. Ellison, *ACS Sustainable Chem. Eng.*, 2020, **8**, 12036–12044.
26 H. Jeong, S.-J. Hong, J. S. Yuk, H. Lee, H. Koo, S. H. Park and J. Shin, *ACS Sustainable Chem. Eng.*, 2023, **11**, 4871–4884.
27 C. Xu, L. Wang, Y. Liu, H. Niu, Y. Shen and Z. Li, *Macromolecules*, 2023, **56**, 6117–6125.
28 S. Liang, C. J. Ellison and M. A. Hillmyer, *Polym. Chem.*, 2025, **16**, 3511–3522.
29 S. Liang, D. M. Krajovic, B. D. Hoehn, C. J. Ellison and M. A. Hillmyer, *ACS Appl. Polym. Mater.*, 2025, **7**, 1411–1420.
30 X. Xia, R. Suzuki, K. Takojima, D.-H. Jiang, T. Isono and T. Satoh, *ACS Catal.*, 2021, **11**, 5999–6009.
31 T. T. D. Chen, L. P. Carrodeguas, G. S. Sulley, G. L. Gregory and C. K. Williams, *Angew. Chem., Int. Ed.*, 2020, **59**, 23450–23455.
32 G. S. Sulley, G. L. Gregory, T. T. D. Chen, L. P. Carrodeguas, G. Trott, A. Santmarti, K. Y. Lee, N. J. Terrill and C. K. Williams, *J. Am. Chem. Soc.*, 2020, **142**, 4367–4378.
33 Z. Zhou, X. Wang, S. Liu, T. Lang, S. Cheng, X. Pang, X. Chen and X. Wang, *ChemSusChem*, 2025, **18**, e202402546.
34 A. Beharaj, I. Ekladious and M. W. Grinstaff, *Angew. Chem., Int. Ed.*, 2019, **58**, 1407–1411.
35 A. Beharaj, E. Z. McCaslin, W. A. Blessing and M. W. Grinstaff, *Nat. Commun.*, 2019, **10**, 5478.
36 A. C. Deacy, G. L. Gregory, G. S. Sulley, T. T. D. Chen and C. K. Williams, *J. Am. Chem. Soc.*, 2021, **143**, 10021–10040.

37 Y.-Y. Zhang, G.-W. Yang, R. Xie, X.-F. Zhu and G.-P. Wu, *J. Am. Chem. Soc.*, 2022, **144**, 19896–19909.
38 N. V. Reis, A. C. Deacy, G. Rosetto, C. B. Durr and C. K. Williams, *Chem. – Eur. J.*, 2022, **28**, e202104198.
39 W. T. Diment, W. Lindeboom, F. Fiorentini, A. C. Deacy and C. K. Williams, *Acc. Chem. Res.*, 2022, **55**, 1997–2010.
40 C. A. L. Lidston, S. M. Severson, B. A. Abel and G. W. Coates, *ACS Catal.*, 2022, **12**, 11037–11070.
41 K. H. S. Eisenhardt, F. Fiorentini, F. Butler, R. Thorogood and C. K. Williams, *ACS Catal.*, 2025, **15**, 12959–12983.
42 T. T. D. Chen, Y. Zhu and C. K. Williams, *Macromolecules*, 2018, **51**, 5346–5351.
43 A. J. Kinloch, *Adhesion and Adhesives*, Springer Dordrecht, 1st edn, 1987.
44 T. Stößer, D. Mulryan and C. K. Williams, *Angew. Chem., Int. Ed.*, 2018, **57**, 16893–16897.
45 C. Romero-Guido, I. Belo, T. M. N. Ta, L. Cao-Hoang, M. Alchihab, N. Gomes, P. Thonart, J. A. Teixeira, J. Destain and Y. Waché, *Appl. Microbiol. Biotechnol.*, 2011, **89**, 535–547.
46 P. Olsén, T. Borke, K. Odelius and A.-C. Albertsson, *Biomacromolecules*, 2013, **14**, 2883–2890.
47 M. Winkler, C. Romain, M. A. R. Meier and C. K. Williams, *Green Chem.*, 2015, **17**, 300–306.
48 S. Wu, Y. Zhou, D. Gerngross, M. Jeschek and T. R. Ward, *Nat. Commun.*, 2019, **10**, 5060.
49 E. Mahmoud, D. A. Watson and R. F. Lobo, *Green Chem.*, 2014, **16**, 167–175.
50 S. Giarola, C. Romain, C. K. Williams, J. P. Hallett and N. Shah, *Chem. Eng. Res. Des.*, 2016, **107**, 181–194.
51 G. L. Gregory, G. S. Sulley, L. P. Carrodeguas, T. T. D. Chen, A. Santmarti, N. J. Terrill, K.-Y. Lee and C. K. Williams, *Chem. Sci.*, 2020, **11**, 6567–6581.
52 C. Gao, K. C. Poon, M. Concilio, T. Zinn, G. L. Gregory and C. K. Williams, *Adv. Mater.*, 2025, **37**, 2416674.
53 K. C. Poon, G. L. Gregory, G. S. Sulley, F. Vidal and C. K. Williams, *Adv. Mater.*, 2023, **35**, 2302825.
54 A. Spyros, D. S. Argyropoulos and R. H. Marchessault, *Macromolecules*, 1997, **30**, 327–329.
55 T. Stößer, T. T. D. Chen, Y. Zhu and C. K. Williams, *Phil. Trans. R. Soc., A*, 2018, **376**, 20170066.
56 Z. Xie, Z. Yang, C. Hu, F.-Q. Bai, N. Li, Z. Wang, S. Ku, X. Pang, X. Chen and X. Wang, *J. Am. Chem. Soc.*, 2025, **147**, 12115–12126.
57 N. Jannsen, K. C. Poon, A. Craze, C. Gao and C. K. Williams, *Angew. Chem., Int. Ed.*, 2025, **64**, e202505070.
58 G. Si, L. Zhang, B. Han, Z. Duan, B. Li, J. Dong, X. Li and B. Liu, *Polym. Chem.*, 2015, **6**, 6372–6377.
59 H. Li, H. Luo, J. Zhao and G. Zhang, *Macromolecules*, 2018, **51**, 2247–2257.
60 M. T. Martello, D. K. Schneiderman and M. A. Hillmyer, *ACS Sustainable Chem. Eng.*, 2014, **2**, 2519–2526.
61 E. P. Chang, *J. Adhes.*, 1991, **34**, 189–200.
62 E. P. Chang, *J. Adhes.*, 1997, **60**, 233–248.
63 A. Roos and C. Creton, *Macromolecules*, 2005, **38**, 7807–7818.

